PIDAT - A Computer Program for Implant Diffusion And Trapping

W. Möller

IPP 9/44 November 1983

MAX-PLANCK-INSTITUT FÜR PLASMAPHYSIK

8046 GARCHING BEI MÜNCHEN

MAX-PLANCK-INSTITUT FÜR PLASMAPHYSIK

GARCHING BEI MÜNCHEN

PIDAT - A Computer Program for Implant Diffusion And Trapping

W. Möller

IPP 9/44 November 1983

Die nachstehende Arbeit wurde im Rahmen des Vertrages zwischen dem Max-Planck-Institut für Plasmaphysik und der Europäischen Atomgemeinschaft über die Zusammenarbeit auf dem Gebiete der Plasmaphysik durchgeführt.

IPP 9/44 W. Möller PIDAT - A Computer Program for Implant Diffusion And Trapping

November 1983

Abstract

A finite-difference computer program is described which has been written to treat diffusion and trapping problems in ion implantation and plasma-wall interaction applications.

The one-dimensional code employs a nonequidistant, exponentially varying mesh grid, the numerical approximation on which is only precise to order Δx. Examples, however, show this inaccuracy to be negligible for practical problems.

Representative results for deuteron implantations into stainless steel are compared to analytical predictions. The role of simplified source distributions is discussed.

Contents

I. INTRODUCTION

Many problems in the field of ion implantation are influenced by bulk diffusion and the interaction of the implanted atoms with traps. A recent interest in the phenomena associated with hydrogen implantation arose especially in the field of fusion research /1-3/. In fusion devices making use of magnetic plasma confinement, high fluxes of neutral hydrogen atoms will bombard the first wall of the vessel, the release, retention and permeation of which play an important role for the machine operation and, in particular for the tritium isotope, safety aspects.

In order to describe these phenomena mathematically, one has to solve the diffusion equation with a source term representing the depth distribution of the implanted atoms after coming to rest, and with boundary conditions which generally account for the reemission of hydrogen from the surface in molecular form, i.e. after recombining from the - in general - atomic bulk solution and surface adsorption states. Furthermore, a trapping and detrapping term has to be included, as hydrogen atoms are often bound to local traps with an enthalpy exceeding the activation energy for interstitial diffusion. These traps can be either pre-existant due to bulk impurities or defects, e.g., from mechanical deformation, or ion-induced due to damage created by implanted ions /4-6/.

The complexity of the source and trapping terms and of the boundary conditions recommends and often requires the use of numerical methods for the present problem, though analytical solutions can be given under simplifying assumptions /7-9/. Numerical codes have been set up by a number of authors /10-13/. Of these, the DIFFUSE /12/ and PERI /13/ codes have been frequently used in plasma-wall interaction studies. Both these codes are subject to limitations which are due to a general difficulty in the

numerical treatment of implantation problems, which arises in particular for permeation calculations: The thickness of the implanted material is in general much larger than that of the implanted region; for the latter, however, a sufficient resolution of spatial mesh points is required. A special combination of equidistant meshpoints in the implanted layer and nonequidistant ones throughout the bulk of the target is employed in DIFFUSE; this might cause discontinuities of the results at the depth of transition /14/. PERI always assumes a delta-function source at the surface restricting its applicability to certain cases (see Sect. 5).

To avoid the problems mentioned before, the PIDAT program employs a continuously varying exponential mesh grid. It has originally been set up by the author at the university of Bochum, FRG, and made available to the AMDAHL-470 and CRAY-1 computers at the Max-Planck-Institut für Plasmaphysik. The program has been applied in the past successfully for problems of hydrogen and helium implantation /6,15/.

In the present report, first the basic equations and boundary conditions will be listed, together with simple analytic approximations and solutions. Subsequently, the finite-difference approximation will be discussed to some detail. After a section which describes the input and output data for a standard version, finally some examples and comparisons will be given on plasma-wall problems.

2. BASIC EQUATIONS AND BOUNDARY CONDITIONS

For the given problem, a solution of the diffusion equation including a source term and a trap term is required. It is sufficient to treat the problem one-dimensionally, as long as the lateral expansion of the implanted area is large compared to the thickness under consideration. As in the standard version of PIDAT, we assume an homogeneous host material and only one implanted and diffusing species, but allow for n_T different types of traps. The total concentration of foreign atoms is composed of solute and trapped fractions

$$c(x,t) = c_s(x,t) + \sum_{j=1}^{n_T} c_j(x,t) \qquad (1)$$

as function of depth x and time t. In the following, all concentrations, fluxes and areal densities will be taken in atomic units, i.e. relative to the host atomic density C_H. Then according to Fick's law for a plane geometry:

$$\frac{\partial c_s}{\partial t} = D \frac{\partial^2 c_s}{\partial x^2} - \sum_{j=1}^{n_T} T_j (c_s, c_j; x, t) + S(x,t) , \qquad (2)$$

where T_j and S denote the trap terms and the source function, respectively. Accordingly,

$$\frac{\partial c_j}{\partial t} = T_j(c_s, c_j; x, t) . \qquad (3)$$

The trapping terms are composed from a capture rate and a release rate /16/ both of which are controlled by diffusion /17/. For the case of permanent and isolated traps with a local concentration being small compared to the host atomic density, it can be written as /18/:

$$T_j = 4\pi\, r_j\, C_H\, D\, [c_s\, (c_j^T - c_j) - c_j z_j e^{-U_j/kT}]. \qquad (4)$$

In eq. (4), r_j denotes an effective trap radius, z_j a coordination number (the number of solute sites adjacent to a trap through which a released atom may escape), and U_j the binding enthalpy. The traps are assumed to saturate at a local concentration $c_j = c_j^T$, $c_j^T(x)$ denoting the trap concentration. Together with the Arrhenius relation for the diffusion coefficient,

$$D = D_o\, e^{-U_d/kT}, \qquad (5)$$

the activation energy for release from a trap amounts to $(U_j + U_d)$. Trapping terms similar to eq. (4) have been proposed by different authors /7, 19/; as the results of the calculations are mainly determined by the given activation energies and trap concentrations, differences in the factors of eq. (4) are generally of negligible influence. Different trap terms for larger precipitates have also been proposed /6, 11/.

The boundary conditions (for the target surface x=0 and the rear surface, or a given depth, x=d) are chosen according to the model of Baskes /20/. The flux of diatomic molecules, which leaves the surface after recombination, is given by

$$j_- = K_r [c_s(x=0)]^2, \qquad (6)$$

with the recombination constant

$$K_r = C_H \frac{K_o}{\sqrt{T}}\, e^{-U_o/kT} \qquad (7)$$

The activation energy U_o and the preexponential factor K_o can be calculated in a simple way from the diffusion and solution data /20/. The boundary condition (6) contains the limiting cases of the impermeable surface (K_r=0) and the ideally permeable surface ($K_r \to \infty$).

With eq. (6) and

$$j = - D \frac{\partial c_s}{\partial x} \tag{8}$$

the boundary condition for x=0 is (similar for x=d)

$$\left.\frac{\partial c_s}{\partial x}\right|_{x=0} = \frac{K_r}{D}[c_s(x=0)]^2 \ . \tag{9}$$

Under certain circumstances, e.g. for very shallow implantations, the problem can be simplified by approximating the depth-dependent source term of eq. (2) by a delta function at the surface, i.e. $S(x) = j_o \delta(x)$ with the incident flux j_o (j_o will always represent the nonreflected fraction of the incident beam flux). The conservation of fluxes then requires in generalization of eq. (9)

$$\left.\frac{\partial c_s}{\partial x}\right|_{x=0} = \frac{1}{D}\,[K_r(c_s(x=0))^2 - j_o]. \tag{1o}$$

3. ANALYTICAL CONCEPTS

Analytical solutions of the above equations are only possible in simple cases. For example, an exact solution can be derived by, e.g., Laplace-transform techniques /21/, in the absence of traps for an ideally permeable surface, i.e. $c_s(0) = 0$, and a delta function source term, i.e. $S(x) = j_o \delta(x-R)$ at the mean range R. The solution for a semiinfinite medium is given by:

$$c_s(x,t) = - \frac{j_o}{2D}\,[2(\frac{Dt}{\pi})^{1/2}(e^{-\frac{(R+x)^2}{4Dt}} - e^{-\frac{(R-x)^2}{4Dt}}) \tag{11}$$

$$-(R+x)\,\mathrm{erfc}\,\frac{R+x}{\sqrt{4Dt}} + (R-x)\,\mathrm{erfc}\,\frac{R-x}{\sqrt{4Dt}}]$$

for $x \leq R$ and

$$c_s(x,t) = -\frac{j_o}{2D}\left[2\left(\frac{Dt}{\pi}\right)^{1/2}\left(e^{-\frac{(R+x)^2}{4Dt}} - e^{-\frac{(R-x)^2}{4Dt}}\right)\right. \tag{12}$$

$$\left. - (R+x)\,\mathrm{erfc}\,\frac{R+x}{\sqrt{4Dt}} - (R-x)\,\mathrm{erfc}\,\frac{x-R}{\sqrt{4Dt}}\right]$$

for $x \geq R$.

The calculation of permeation problems requires a finite medium and leads to an even more complicated calculation. Here, only the result for the atomic flux leaving the rear ("downstream") surface of a sample of thickness d shall be given for later comparisons:

$$j_+ = j_o \frac{R}{d}\left(1 + \frac{2d}{\pi R}\sum_{k=1}^{\infty}\frac{(-1)^k}{k}\sin\frac{\pi kR}{d}\, e^{-\frac{\pi^2 Dk^2}{d^2}t}\right) \tag{13}$$

It is often helpful to study the asymptotic behaviour with respect to time. This can even be done including the correct boundary conditions (eq. (6)). Still with a delta function at x=R as source term, the stationary situation is depicted by the diagram of Fig. 1. Due to the shallow depths of implantation, the permeating fraction j_+ will in most cases be small compared to the implanted flux, i.e. $j_- \approx j_o$ for the reemitted flux at the upstream side. Then, according to eq. (6):

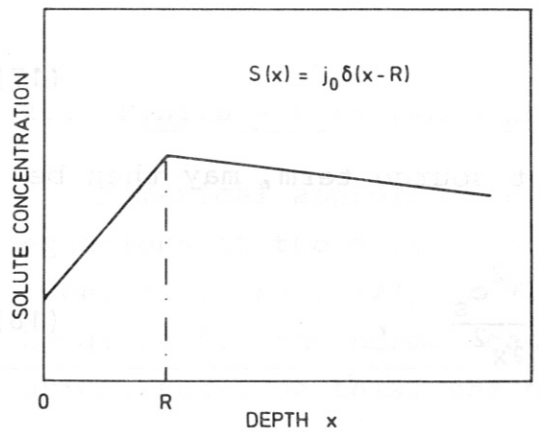

Fig. 1:

Depth profile of the solute concentration in case of an idealized source distribution

$$c_s(0) = \left(\frac{j_o}{K_r}\right)^{1/2} , \tag{14}$$

and

$$c_s(R) = \left(\frac{j_o}{K_r}\right)^{1/2} \left(1 + (j_o K_r)^{1/2} \frac{R}{D}\right) \tag{15}$$

Using the parameter /9/

$$W = (j_o K_r)^{1/2} \cdot \frac{R}{D} \tag{16}$$

one may now distinguish different regimes: $W >> 1$ means $c_s(R) >> c_s(0)$, i.e. the recombination process is fast and the release through the surface is limited by diffusion. $W < 1$ characterizes recombination-limited processes; in the limit of $W << 1$, which is valid for highly exothermal solution behaviour and very fast diffusion, the implant will be distributed homogeneously throughout the whole thickness.

For the situation depicted by Fig. 1, approximate analytic steady-state solutions are given in Ref. /9/.

As a third example for analytical approximations, it shall be shown that the effect of shallow traps with small occupancy may be included into an effective diffusion coefficient /8, 22/. Assuming local equilibrium, which is justified over a wide range of conditions /5/, and for $c_1 << c_1^T$ (for only one type of traps), eq. (4) yields

$$c_1 = c_s \frac{c^T}{z_1} e^{U_1/kT} \tag{17}$$

Equations (2) and (3), without source term, may then be combined to

$$\frac{\partial c_s}{\partial t} = \frac{D}{1 + \frac{c^T}{z_1} e^{U_1/kT}} \frac{\partial^2 c_s}{\partial x^2} , \tag{18}$$

that is, the change of the solute concentration is subject to an effective diffusion coefficient

$$D_{eff} = \frac{D}{1 + \frac{c^T}{z_1} e^{U_1/kT}} \qquad (19)$$

For a trap concentration which is independent on depth, simple analytical solutions will then apply also for the case of shallow traps.

4. NUMERICAL SOLUTION

In the previous section it was demonstrated that the applicability of analytical approximations and solutions is rather limited, so that numerical solutions will be required for a large number of problems. Also, from a practical point of view, numerical evaluations will often be preferable, which, by the availability of fast computers, are often much faster than the evaluation of complicated analytical results. The main advantage of numerical methods is, however, their flexibility with respect to boundary conditions and additional processes, e.g. different trapping terms for the present problem.

4.1 Finite - Difference Scheme

Numerical approximations to partial differential equations of the diffusion type have been known for long (see, e.g., ref. /23/).Here, only the main results will be given for the normal case of equidistant spatial mesh grids. Based on this, the non-equidistant approximation

used in PIDAT will be derived and described in detail.

For the one-dimensional problem and a plane geometry, the target (or its region of interest) is commonly divided into (n-1) slabs of equal thickness Δx, starting at $x(1) = 0$ and ending at $x(n) = d$. For any function of the depth, $f(x)$, its value at the mesh point $x(i+1)$ is given by the Taylor-expansion

$$f(i+1) = f(i) + \Delta x \left.\frac{\partial f}{\partial x}\right|_{x(i)} + \frac{\Delta x^2}{2} \left.\frac{\partial^2 f}{\partial x^2}\right|_{x(i)} + O(\Delta x^3) + O(\Delta x^4) + \ldots \qquad (20)$$

With the similar expansion for $f(i-1)$, one obtains

$$\left.\frac{\partial f}{\partial x}\right|_{x(i)} = \frac{f(i+1) - f(i-1)}{2\ \Delta x} + O(\Delta x^2) \qquad (21)$$

and

$$\left.\frac{\partial^2 f}{\partial x^2}\right|_{x(i)} = \frac{f(i+1) - 2\ f(i) + f(i-1)}{\Delta x^2} + O(\Delta x^2), \qquad (22)$$

i.e. approximations to the first and second derivatives which are precise to the order (Δx^2), which are both valid for $1 < i < n$.

Defining a non-equidistant mesh grid according to the recursion relation

$$x(i+1) = x(i) + \Delta x(i), \qquad (23)$$

the above procedure yields:

$$\left.\frac{\partial f}{\partial x}\right|_{x(i)} = \frac{1}{\Delta x(i)+\Delta x(i-1)} [f(i+1) - f(i-1) - \left(\frac{\Delta x(i)^2}{2} - \frac{\Delta x(i-1)^2}{2}\right) \left.\frac{\partial^2 f}{\partial x^2}\right|_{x(i)} - \left(\frac{\Delta x(i)^3}{6} + \frac{\Delta x(i-1)^3}{6}\right) \left.\frac{\partial^3 f}{\partial x^3}\right|_{x(i)}] + O(\Delta x^2) \qquad (24)$$

$$\left.\frac{\partial^2 f}{\partial x^2}\right|_{x(i)} = \frac{2}{\Delta x(i)^2+\Delta x(i-1)^2}\,[f(i+1)-2f(i)+f(i-1)$$

$$- (\Delta x(i) - \Delta x(i-1))\left.\frac{\partial f}{\partial x}\right|_{x(i)} \qquad (25)$$

$$- \left(\frac{\Delta x(i)^3}{6} - \frac{\Delta x(i-1)^3}{6}\right)\left.\frac{\partial^3 f}{\partial x^3}\right|_{x(i)}] + O(\Delta x^2)$$

Inserting eqs. (24) and (25) into each other and neglecting the cubic terms, one obtains

$$\left.\frac{\partial f}{\partial x}\right|_{x(i)} = \frac{1}{\Delta x(i) + \Delta x(i-1)}\,\left[\frac{\Delta x(i-1)}{\Delta x(i)}\,(f(i+1)-f(i))\right.$$

$$\left. + \frac{\Delta x(i)}{\Delta x(i-1)}\,(f(i) - f(i-1))\right] \qquad (26)$$

and

$$\left.\frac{\partial^2 f}{\partial x^2}\right|_{x(i)} = \frac{2}{\Delta x(i)+\Delta x(i-1)}\,\left[\frac{f(i+1)}{\Delta x(i)} - \left(\frac{1}{\Delta x(i)} + \frac{1}{\Delta x(i-1)}\right)f(i)\right.$$

$$\left. + \frac{f(i-1)}{\Delta x(i-1)}\right] \qquad (27)$$

The cubic terms, which correspond to a term of order Δx in eqs. (26) and (27), vanish only for $\Delta x(i) = \Delta x(i-1)$, i.e. the equidistant case. Thus, a "nonequidistant" approximation is only precise to the order Δx rather than Δx^2 for the equidistant one, so that any results have to be carefully checked with respect to the influence of this approximation.

For PIDAT, an exponentially varying mesh grid is employed with

$$x(1) = 0 \tag{28}$$

and

$$\Delta x(i) = e^{(i-1)\alpha} \cdot \Delta x_o \ , \tag{29}$$

with an 'expansion coefficient' α and the subsurface mesh width Δx_o. Accordingly, the nodes are

$$x(i) = \frac{e^{(i-1)\alpha}-1}{e^{\alpha} - 1} \ \Delta x_o \ . \tag{30}$$

From eq. (30), Δx_o may be calculated with given $d = x(n)$ and α:

$$\Delta x_o = \frac{e^{\alpha} - 1}{e^{(n-1)\alpha}-1} \ d. \tag{31}$$

With eq. (29), the spatial derivatives of the solute concentration become

$$\left.\frac{\partial c_s}{\partial x}\right|_{x(i)} = \frac{1}{2\Delta x_o \cosh\frac{\alpha}{2}} \left[\frac{c_s(i+1)-c_s(i)}{e^{(i-1/2)\alpha}} + \frac{c_s(i)-c_s(i-1)}{e^{(i-5/2)\alpha}}\right] \tag{32}$$

and

$$\left.\frac{\partial^2 c_s}{\partial x^2}\right|_{x(i)} = \frac{1}{\Delta x_o^2 \cosh\frac{\alpha}{2}} \left[\frac{c_s(i+1)-c_s(i)}{e^{(2i-5/2)\alpha}} + \frac{c_s(i-1)-c_s(i)}{c^{(2i-7/2)\alpha}}\right] . \tag{33}$$

Whereas eq. (33) can be directly inserted into the diffusion equation for $1 < i < n$, the boundary conditions (eqs. (9) and (10)) require an additional treatment. At the surface with $x(1) = 0$, an artificial external node $x(0)$ is defined. The general boundary condition (eq. (10)) then reads

$$K_r (c_s(1))^2 - j_o = \frac{D}{2\Delta x_o \cos h\frac{\alpha}{2}} \left[\frac{c_s(2)-c_s(1)}{e^{\alpha/2}} + \frac{c_s(1)-c_s(0)}{e^{-3/2\alpha}}\right] \tag{34}$$

from which

$$\frac{c_s(0)}{e^{-3/2\alpha}} = -\frac{2\Delta x_o \cosh\frac{\alpha}{2}}{D}\left[K_r(c_s(1))^2 - j_o\right] + \frac{c_s(2)-c_s(1)}{e^{\alpha/2}} + \frac{c_s(1)}{e^{-3/2\alpha}} \cdot \qquad (35)$$

Inserting eq. (35) into eq. (33) with i=1, one obtains finally

$$\left.\frac{\partial^2 c_s}{\partial x^2}\right|_{x(1)} = \frac{2}{\Delta x_o^2}\left[c_s(2)-c_s(1) - \frac{\Delta x_o}{D}\left(K_r(c_s(1))^2-j_o\right)\right], \qquad (36)$$

and, correspondingly for the downstream surface, x(n) = d:

$$\left.\frac{\partial^2 c_s}{\partial x^2}\right|_{x(n)} = \frac{2}{\Delta x_o^2} \cdot \frac{1}{e^{(2n-4)\alpha}}\left[c_s(n-1) - c_s(n) + e^{(n-2)\alpha}\,\frac{\Delta x_o}{D} \cdot K_r(c_s(n))^2\right] . \qquad (37)$$

4.2 Integrator Routine

With the numerical approximations given by eqs. (33), (36) and (37), the extended diffusion equation system (2) and (3) can now be solved. Standard methods of solving equation systems of this type can be found in the literature /23/. It is advisable, however, to employ a well-tested integrator routine from a suitable program library. For the present purpose, the program package GEARB /11, 24/ is employed, which provides solutions for systems of ordinary differential equations with band structure (see below) with selfadjusted step sizes to guarantee stability.

By means of the finite-difference approximations, the partial differential equation system (2) and (3) is converted into a system of ordinary differential equations of rank $n \cdot (n_t+1)$, by setting

$$y((i-1)n_t+i) = c_s(i) \tag{38}$$

and

$$y((i-1)n_t + i+j) = c_j(i). \tag{39}$$

As only the concentrations at up to the first neighbouring nodes contribute to each equation, the resulting equation system

$$\dot{\vec{y}} = A \cdot \vec{y} \tag{40}$$

is of banded structure, i.e. the matrix A contains zero coefficients except for a band of width $(2n_t+3)$ around the main diagonal. This is compatible with the GEARB integrator package.

The GEARB routines are especially suited for 'stiff' problems, i.e. problems with widely varying time constants, for which the terms with the smaller time constants have already decayed to insignificant levels. Diffusion in a medium containing traps represents such a problem, as, for example, a local equilibrium may be achieved very quickly (see Sect. 3), whereas long times may be required to establish stationary situations during implantation, or especially permeation experiments.

5. USE OF PIDAT

Besides the quantities defined in Sect. 2, PIDAT has to be supplied with an initial distribution $\vec{y}(t=0)$. In the basic version of PIDAT, PIDVC, the input stream of which is also described in App. B, either a solute distribution, $c_s(t=0)$, or a trapped distribution $c_j(t=0)$ may be defined, the other components being zero.

As well as the source distribution, $S(x)$, and the trap distributions, $c_j^T(x)$, the initial distribution may either be defined as a Gaussian function or as an arbitrary data set. The complete initial distribution $\vec{y}$ may also be taken as a dump file from a previous PIDAT calculation.

The normalization of the source distribution is performed internally to a given flux j_o of nonreflected atoms. Furthermore, as a simple time dependence of the source function,

$$S(x,t) = \frac{S(x)}{2} \left[1-\mathrm{erf}\left(\frac{t-t_o}{\sigma}\right)\right] , \qquad (41)$$

is included, with the 'cutoff' time t_o and a smoothing parameter σ. In particular, a sudden stop of the implantation is simulated with $\sigma << t_o$. The source term is set to zero if the extended boundary condition, eq. (10), is required.

Each run starts at the time t=0 and ends at a given time $t = t_{max}$. In order to apply the program also for thermal desorption problems, the temperature (assumed to be homogeneous) is allowed to ramp linearly as function of the time:

$$T = T_o + \beta\, t \qquad (42)$$

The program outputs, after present time steps, the complete profiles, $c_s(x)$ and $c_j(x)$, the particle fluxes emitted through both surface and the corresponding total fluences,

and the individual depth integrals of c_s and c_j as well as the total bulk integral. The integration may either be performed up to a maximum depth or according to an arbitrary weighting function defined by an input data set.

An additional control output contains the performance report including a list of the current GEARB step size, the surface fluxes and the total bulk integral.

The GEARB results are precise to a preset number ε, denoting the single-step error in y_i. The internal time step size is adjusted by GEARB between 10^{-10} and 10^{2} of a preset initial step size, Δt_o. If an increment less than $10^{-10}\ \Delta t_o$ is required, the program will be aborted. The user is informed on the reduction of step sizes on the control output.

Any error conditions met in GEARB will be reported by their error code (App. A) before the program is aborted.

The GEARB package allows to choose between different methods of solving the differential equation system, by means of a method flag

$$m_f = 10 \cdot m_{meth} + m_{iter} \quad . \tag{43}$$

m_{meth} is the basic method indicator, with $m_{meth} = 1$ for implicit Adams methods and $m_{meth} = 2$ for backward differentiation formulas. Different m_{meth} may be adequate for different problems or even in different subintervals of a problem /24/; $m_{meth} = 2$, however, has been found to work best for problems of the kind described in Sect. 5.
m_{iter} is the corrector iteration method switch /24/, with $m_{iter} = 0$ for functional iteration, 1 for chord method with user-supplied Jacobian matrix $(\partial \dot{y}_k / \partial y_i)$, 2 for chord method with Jacobian generated internally, and 3 for chord method with diagonal approximation to Jacobian. Of these, $m_{iter} = 0$ is least effective. $m_{iter} = 1$ has been found to

be only insignificantly more effective than $m_{iter} = 2$ at the expense of an often complicated coding of the Jacobian; therefore, $m_{iter} = 1$ has been excluded for PIDVC. For certain problem with a diagonal-dominated Jacobian, $m_{iter} = 3$ may be most effective.

More detailed information on the use of GEARB can be obtained from Ref. /24/.

The standard version of PIDAT, PIDVC, is run on the CRAY-1 computer. Typical computing times for problems like those of Sect. 5 are several seconds. An example of a batch submit file is given in App. C.

6. EXAMPLES

In the present section, some examples will be given for deuterium implantations into stainless steel (304 LN). Diffusion and recombination data are taken according to present knowledge /25/ ($D_o = 2 \cdot 10^{-3}$ cm^2/s , $U_d = 0.535$ eV, $C_H K_o = 2.29 \cdot 10^7$ cm K$^{1/2}$/s, $U_o = 0.428$ eV). The numerical results will be compared to analytical results given in Sect. 3. Furthermore, the influence of the extended boundary condition (eq. (10)) will be demonstrated.

Let us first assume a deuterium flux of $1 \cdot 10^{16}$/cm$^2 \cdot$ s to be implanted into 304 LN stainless steel at an energy of 10 keV, corresponding to a mean range of $R \simeq 7 \cdot 10^{-6}$ cm. Trapping effects shall be neglected. The dependence of the W-parameter (eq. (16)) on temperature is displayed in Fig.2; at room temperature, the system is clearly diffusion-controlled ($W >> 1$). Therefore, the idealised analytical solutions of eqs. (11) and (12) should be applicable. Figure 3 compares the analytical results with those of different PIDAT com-

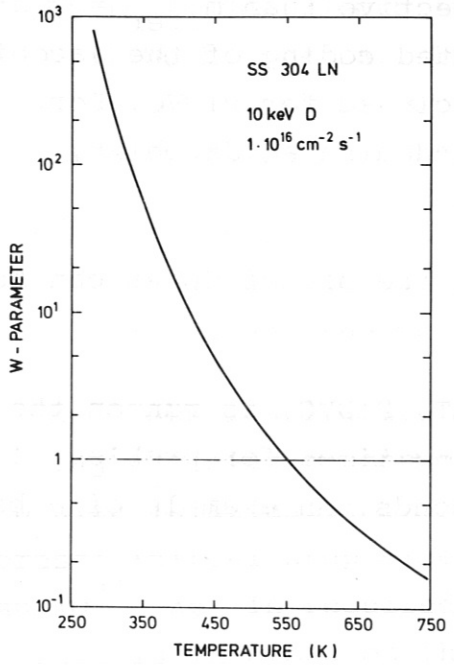

Fig. 2:

Kinetic parameter W (eq. (16)) as function of temperature.

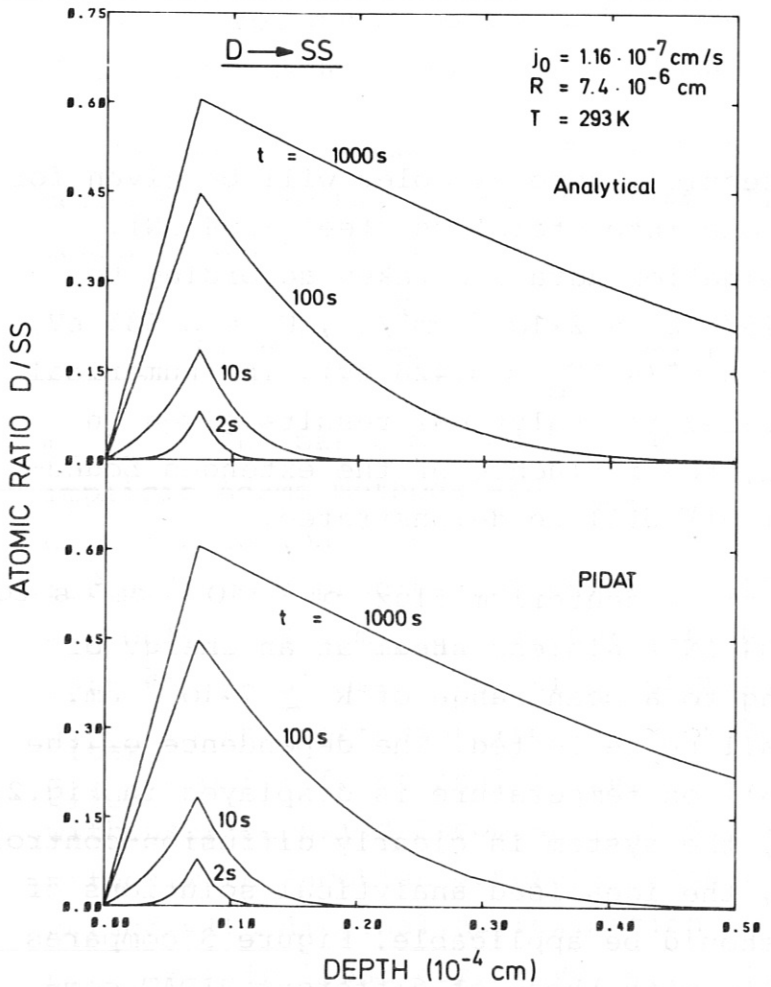

Fig. 3:

Solute concentration profiles at different times from the beginning of implantation for an idealized source $S(x) = j_o \, \delta(x-R)$. The PIDAT calculations have been performed at a sample thickness of 0.5 cm with 100 mesh grid intervals, and $\alpha = 0.15$.

putations. Except for the structure given by the mesh-grid in the PIDAT results, all profiles are identical within the precision of the drawing.

As mentioned above (Sect. 4.1), the nonequidistant mesh grid causes an additional error in the numerical approximation compared to an equidistant grid. With the interval increment parameter α (eq. (29)) being a measure for non-equidistance, the results have to be checked therefore with respect to the dependence on the choice of α.

For the calculations carried out for Fig. 4, an approximate realistic source function (Gaussian according to Ref. /26/) has been chosen rather than a δ-function. It is seen that even large variations of α (corresponding to surface intervals of $\Delta x_o = 1.32 \cdot 10^{-16}$ cm to $\Delta x_o = 2.48 \cdot 10^{-8}$ cm) do not change the profiles, except for the mesh-grid structure.

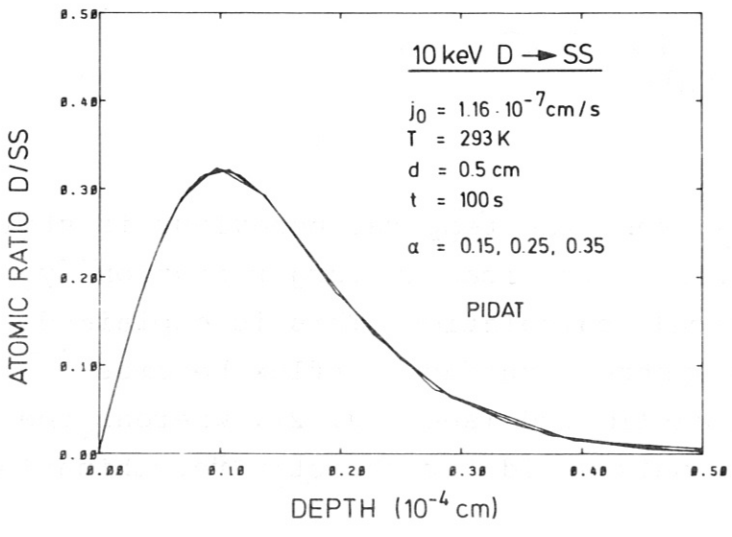

Fig. 4:
Solute concentration profiles for different increment parameters, α. The source distribution was taken from the tabulations of Andersen and Ziegler /26/ as Gaussian with $\bar{R} = 7.2 \cdot 10^{-6}$ cm, $\sigma = 5.2 \cdot 10^{-6}$ cm.

The following example (Fig. 5) describes the permeation of implanted deuterium atoms through a stainless steel foil, with a δ-function as source term. Satisfactory agreement of the analytical solution (eq. (13)) and the numerical result is obtained at 350 K and still st 375 K.

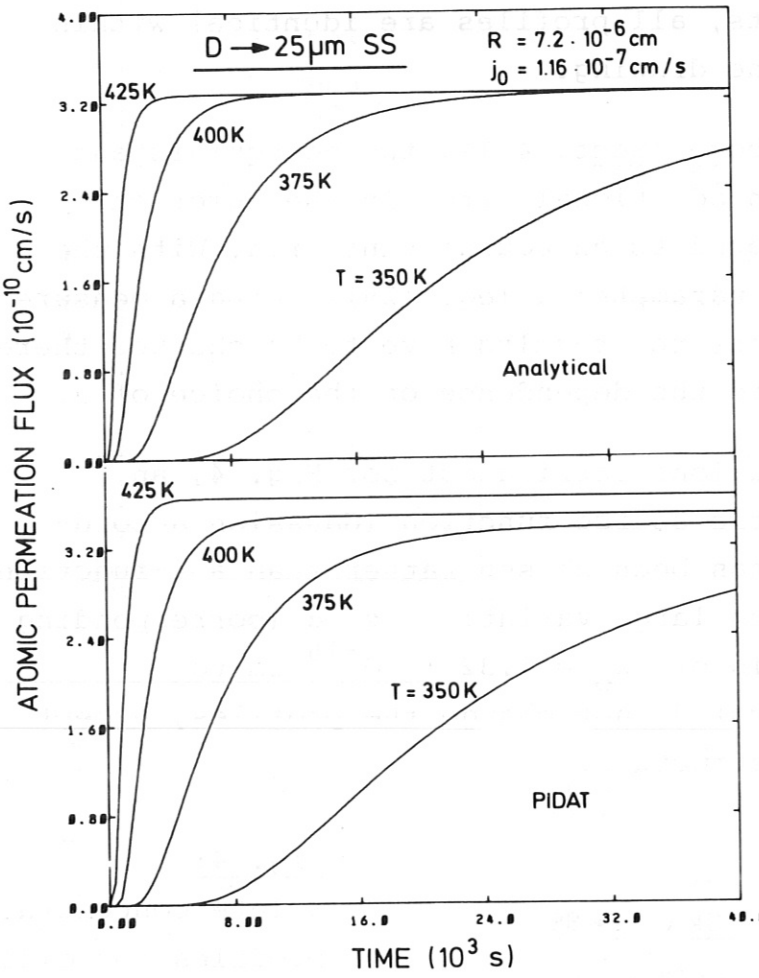

Fig. 5:

Permeation fluxes through a stainless steel foil from analytical and numerical calculations (idealized source, α = 0.08, 100 intervals)

At higher temperatures, the temporal behaviour is still identical, with, however, significantly larger stationary fluxes for the numerical calculation. This is explained by the fact that the upstream surface outflux becomes gradually recombination-limited (see Fig. 2), whereas the analytical formula is only valid for strictly recombination-limited kinetics.

Figure 6 confirms that the result for the permeation problem is also independent of the choice of α. For α = 0.02, Δx_o amounts to $8 \cdot 10^{-6}$ cm, which is close to the mean range. Correspondingly, the deviation for α = 0.02 results from a too coarse grid within the source range.

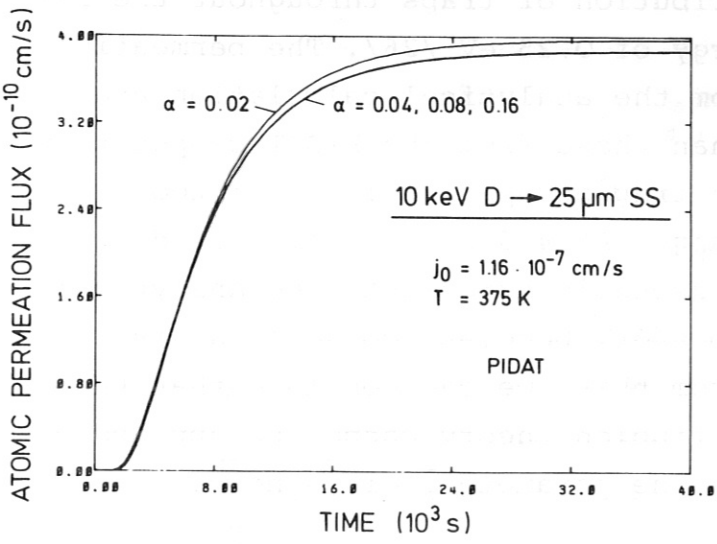

Fig. 6:

Influence of different increment parameters on the permeation fluxes. Source distributions were taken according to Fig. 4, calculations were performed with 100 intervals.

The validity of the effective-diffusion approximation (eqs. (11), (12) and (19)) is investigated in Fig. 7 for

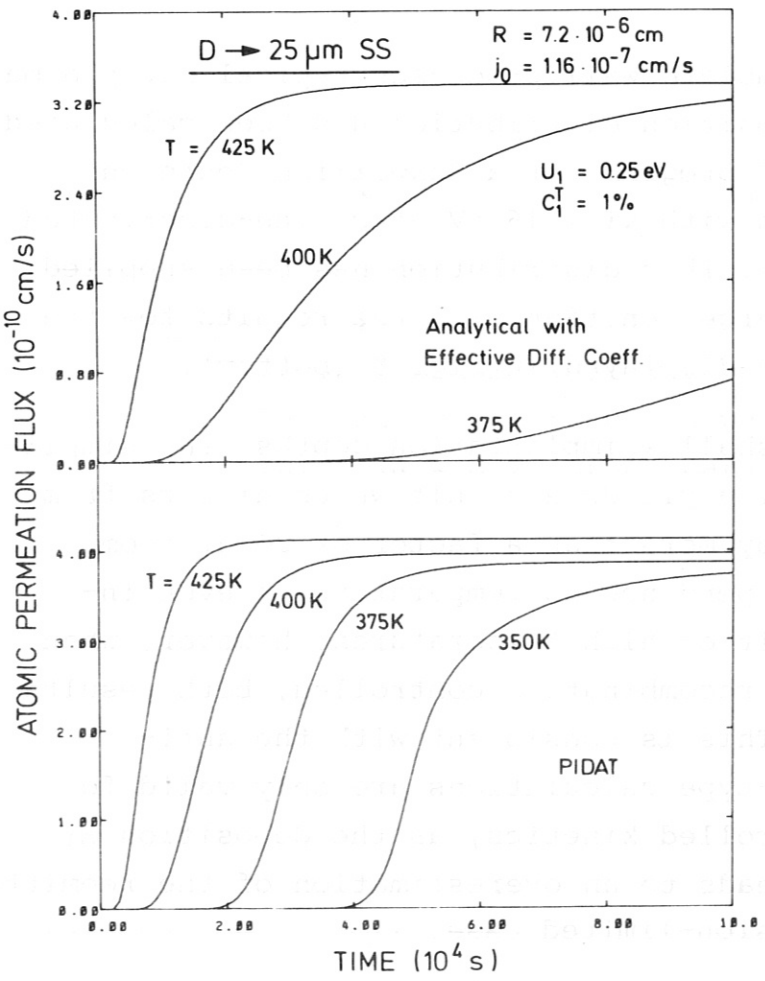

Fig. 7:

Permeation fluxes through a foil with 1 % traps of 0.25 eV binding energy from effective-diffusion theory and PIDAT, the latter with additional parameters according to Fig. 6 and α = 0.08. (Note different ordinate scales!)

a homogeneous distribution of traps throughout the foil with a binding energy of 0.25 eV /26/. The permeation fluxes obtained from the analytical calculation are strongly smaller than those from the PIDAT computation below 425 K, as the trap occupation is still too high in this temperature range. At 425 K, the temporal dependences are in reasonable agreement; the analytical stationary flux, however, becomes too small as it was discussed above. From this, we can conclude that the simple effective diffusion theory cannot be applied at all to systems with the parameters given here.

In the last example, the influence of a simplified source term shall be studied, which is embedded into the boundary condition at the upstream surface (eq. (10)). This source term is exclusively used in the PERI program /13/.

In order to simulate wall processes typical for plasma experiments, a deposition distribution has been calculated using the TRIM /27/ program for a Maxwellian deuteron energy distribution with kT = 16 eV at cosine-distributed angles of incidence. This distribution has been supplied to PIDAT as the source function with the results for the deuterium inventory displayed in Fig. 8 (bottom).

Even for this shallow implantation depths, the simplified ('PERI') version yields a result which differs from the realistic one by more than a factor of 20 at room temperature. The dependence on temperature is even inverted. In the limit of high temperatures, however, when the system becomes recombination-controlled, both results become identical. This is consistent with the anticipation that PERI-type calculations are only valid for recombination-controlled kinetics, as the deposition at the very surface leads to an overestimation of the reemitted flux for the diffusion-limited case.

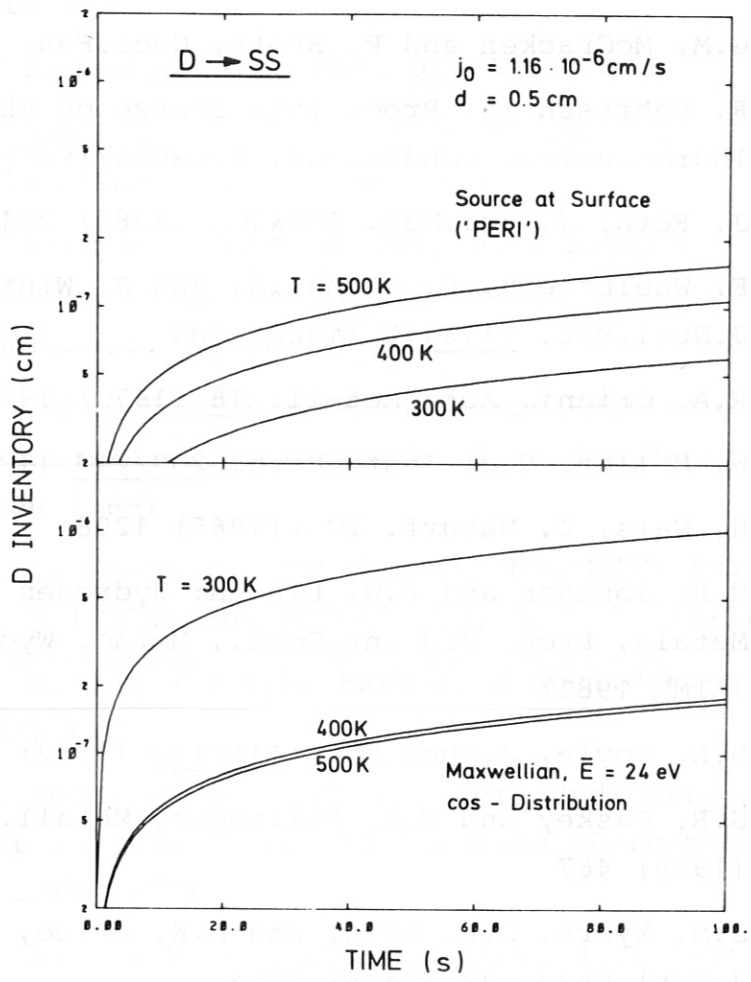

Fig. 8: Calculation of the deuterium inventory for a typical plasma-wall-interaction problem. The source distribution was calculated by TRIM (α = 0.2, other parameters as before).

References

/1/ G.M. McCracken and P. Stott, Nucl.Fus. 19 (1979) 889

/2/ R. Behrisch in: Proc. Int. Course on Physics Close to Thermonuclear Conditions, Varenna/Italy (1980)

/3/ J. Roth, J.Nucl.Mat. 103&104 (1981) 291

/4/ F. Waelbroeck, P. Wienhold, and J. Winter, J.Nucl.Mat. 111&112 (1982) 185

/5/ R.A. Oriani, Acta Metall. 18 (1970) 147

/6/ W. Möller, Nucl.Instr.Meth. 209/210 (1983) 773

/7/ H. Gaus, Z. Naturf. 20 a (1965) 1298

/8/ H.H. Johnson and R.W. Lin in: Hydrogen Effects in Metals, Proc. 3rd Int.Conf., Moran, Wyoming (AIME 1981)

/9/ B.L. Doyle, J.Nucl.Mat. 111&112 (1982) 628

/10/ G.R. Caskey and W.L. Pillinger, Metall.Trans.A6 (1975) 467

/11/ S.M. Myers, D.E. Amos, and D.K. Brice, J.Appl.Phys. 47 (1976) 1812

/12/ M.I. Baskes, Sandia Nat. Laboratories Reports SAND80-8201 (1980) and SAND83-8231 (1983)

/13/ P. Wienhold, M. Profant, F. Waelbroeck, and J. Winter, J.Nucl.Mat. 93&94 (1980) 866

/14/ K.L. Wilson, private communication

/15/ W. Möller, B.M.U. Scherzer, and J. Ehrenberg, J.Nucl.Mat. 111&112 (1982) 669

/16/ A. McNabb and P.K. Foster, Trans.Met.Soc. AIME 227 (1963) 618

/17/ F.S. Ham, J.Phys.Chem.Sol. 6 (1958) 335

/18/ S.M. Myers, Nucl.Instr.Meth. 168 (1980) 265

/19/ K.L. Wilson and M.I. Baskes, J.Nucl.Mat. 74 (1978) 179

/20/ M.I. Baskes, J.Nucl.Mat. 92 (1980) 318

/21/ J. Crank, The Mathematics of Diffusion (Oxford University Press 1975)

/22/ D.J. Mitchell, J.M. Harris, R.C. Patrick, E.P. Boespflug, and L.C. Beavis, J.Appl.Phys. 53 (1982) 970

/23/ W.F. Ames, Numerical Methods for Partial Differential Equations (Th. Nelson & Sons Ltd., London 1969)

/24/ A.C.Hindmarsh, LLL-Reports No. UCID-30001, Rev. 3 (1974) and UCID-30059, Rev. 1 (1975)

/25/ K.L. Wilson and M.I. Baskes, J.Nucl.Mat. 111&112 (1982) 622

/26/ H.H. Andersen and J.F. Ziegler: Hydrogen, Stopping Power and Ranges in All Elements (Pergamon Press, New York 1977)

/27/ J.P. Biersack and L.G. Haggmark, Nucl.Instr.Meth. 174 (1980) 257

Appendix A: GEARB Error Codes

The program will be aborted if one of the following errors occurs:

Code	Meaning
-1	Integration was halted after failing to pass the error test even after reducing the step size, h , by a factor of 10^{10} from its initial value.
-2	Integration was halted after some initial success either by repeated error test failures or by a direct test indicating that EPS is too small.
-3	Integration was halted after failing to achieve corrector convergence even after reducing h by a factor of 10^{10} from its initial value.
-4	An input value was found to be illegal .

Appendix B: PIDVC In/Out Data

The following input data and formats are required for a PIDVC run (the standard version of PIDAT). The individual quantities may easily be correlated to the text of Sections 2 and 4, except for (see eq. (4))

$$BL(j) = 4\pi r_j C_H. \qquad (B\ 1)$$

One type of traps is to be defined at minimum; a calculation without any traps, however, can be performed by putting BL(1) = 0 at one type of traps.

The input stream is subdivided into a parameter data set and several distribution data sets, which are explained below with the corresponding formats given:

```
1. RECORD (5I5):

MF: GEARB METHOD SWITCH (NORMALLY 22)
IOUT: OUTPUT OF INTEGRALS AFTER EACH IOUT'TH TIME STEP
IPR: ADDITIONAL OUTPUT OF PROFILES AFTER EACH IPR'TH TIME STEP
N: NR. OF GRID INTERVALS (EVEN, MAX. 100)
NTR: NR. OF DIFFERENT TYPES OF TRAPS (1 < NTR < 7)

2. RECORD (4E10.4):

H0: INITIAL TIME STEP SIZE
EPS: REQUIRED RELATIVE ACCURACY
TMAXS: SOURCE SWITCHOFF TIME(S)
SIGS: SMOOTHING FOR SOURCE SWITCHOFF (E.G. TMAXS/1E4)

3. RECORD (2I5,4E10.4):

IFR: FRONT SURFACE PERMEABLE(0) OR RECOMBINATION-
     LIMITING WITHOUT(-1) OR WITH(+1) SOURCE TERM
IRE: REAR SURFACE PERMEABLE(0) OR RECOMBINATION-
     LIMITING
RC0: PREEXPON. FACTOR FOR SURFACE RECOMBINATION (CM/S)
AER: CORRESP. ACTIVATION ENERGY (EV)
RC0R, AERR: SAME FOR REAR SURFACE (IF BOTH =0, FRONT SURFACE
            DATA ARE TAKEN)

4. RECORD (4E10.4):

TMAX: LAST VALUE OF TIME (SEC)
DT: INCREASE IN TIME PER STEP (SEC)
AL: EXPANSION COEFFICIENT FOR X-SCALE GRID (0: EQUIDISTANT)
X0: SAMPLE THICKNESS (CM)

5. RECORD (3E10.4):

TMP0: START TEMPERATURE (K)
RATE: LINEAR RAMP CONSTANT (K/SEC)
ALIM: MAX. DEPTH FOR INTEGRATION (CM)

6. RECORD (2E10.4):

DC0: PREEXP. FACTOR OF DIFFUSION (CM2/SEC)
AE: ACTIV. ENERGY OF DIFFUSION (EV)

7. RECORD (6E10.4):

BL(1...NTR): TRAPPING/DETRAPPING RATE FACTOR (CM2)
```

```
8. RECORD (6E1Ø.4):

BM(1...NTR): COORDINATION NUMBER FOR DETRAPPING

9. RECORD (6E1Ø.4):

AET(1...NTR): BINDING ENERGY OF TRAPS (EV)

1Ø. RECORD (3I5):

ISW(1): INITIAL = SOLUTE(1) OR TRAPPED(2...NTR+1) DISTRIBUTION
    IF <Ø, X-Y DATA SET IS READ (XMØ,SØ,CØ,XMAXØ(1) ARE IGNORED)
ISW(2): TRAP CONCENTRATIONS ACCORDING TO PARAMETERS(Ø)
    OR FROM X-Y DATA SET(-1)
ISW(3): SAME FOR SOURCE DISTRIBUTION

11. RECORD (3I5):

JSW: INTEGRATION FROM Ø TO ALIM(Ø) OR ACCORDING TO RELATIVE CROSS
    SECTION ACCORDING TO X-Y DATA SET(-1)
LSW: INPUT OF Y FROM DUMP FILE(-1)
MSW: OUTPUT OF Y TO DUMP FILE BEFORE EXIT(-1)

12. RECORD (4E1Ø.4):

XMØ,SØ,CØ,XMAXØ(1): PARAMETERS OF GAUSSIAN FOR INITIAL
    CONCENTRATION (CENTRAL(CM), STD.DEV.(CM), MAX.CONC.,
    MAX.DEPTH ABOVE WHICH = Ø (CM))

RECORDS NO. 13...(12+NTR) (4E1Ø.4):

XMØ,SØ,CØ,XMAXØ(2...NTR+1): SAME FOR TRAP DISTRIBUTIONS

RECORD NO. (13+NTR) (4E1Ø.4):

XMØ,SØ,CØ,XMAXØ(NTR+2): SIMILAR FOR SOURCE DISTRIBUTION,
    CØ(NTR+2): NONREFLECTED FRACTION OF IMPLANTED FLUX(CM/S),
    I.E. IMPLANTED FLUX DIVIDED BY HOST ATOMIC DENSITY
    IN CASE OF IFR=+1 OR ISW(3)<Ø, XMØ,SØ AND
    XMAXØ(NTR+2) ARE IGNORED


DUMP INPUT IN CASE OF NEGATIVE LSW:
TO BE APPENDED AS FIRST DATA SET AFTER ABOVE INPUT PARAMETERS.
(ISW(1)<Ø IS THEN IGNORED)


INPUT DISTRIBUTIONS IN CASE OF NEGATIVE ISW,JSW:

TO BE APPENDED IN CONSECUTIVE ORDER, CONTAINING ONE HEADLINE
(12 CHAR.) AND UP TO 1ØØ X-Y DATA PAIRS (2E15.6)
```

An example of a parameter data set is given below:

```
  22  1ØØ 5ØØØ  1ØØ    1
Ø.1ØØØE-2 Ø.1ØØØE-7 Ø.1ØØØE+9 Ø.1ØØØE-4
  -1   -1 Ø.229ØE+4 Ø.428ØE+Ø
Ø.1ØØØE+2 Ø.1ØØØE-2 Ø.15ØØE-Ø Ø.5ØØØE-Ø
Ø.293ØE+3 Ø.ØØØØE-2 Ø.5ØØØE-1
Ø.2ØØØE-2 Ø.535ØE+Ø
Ø.4Ø3ØE17
Ø.1ØØØE+1
Ø.24ØØE+Ø
   1    Ø   -1
   Ø   -1    Ø
Ø.85ØØE-5 Ø.388ØE11 Ø.ØØØØE+1 Ø.1ØØØE+1
Ø.143ØE-4 Ø.85ØØE-5 Ø.ØØØØE-1 Ø.5ØØØE-3
Ø.143ØE-4 Ø.85ØØE-5 Ø.132ØE-6 Ø.5ØØØE-3
```

The program output is as follows:

```
PRINTED OUTPUT  (PUNCH FILE):

INTEGRALS:      COLUMN 1: TIME(S)
                       2: TEMPERATURE(K)
                       3: AMOUNT TRANSMITTED THROUGH FRONT SURFACE
                       4: INTEGRAL OF BULK CONCENTRATION
                       5: AMOUNT TRANSMITTED THROUGH REAR SURFACE
                       6: FLUX THROUGH FRONT SURFACE
                       7: FLUX THROUGH REAR SURFACE
                       8: INTEGRAL OF SOLUTE CONCENTRATION
                       9...NTR+8: INTEGR. OF TRAPPED CONCENTR.S

PROFILES:       COLUMN 1: DEPTH(CM)
                       2: TOTAL CONCENTRATION
                       3: SOLUTE CONCENTRATION
                       4...NTR+3: TRAPPED CONCENTRATIONS


CONTROL OUTPUT  (PRINT FILE):

COLUMN 1: TIME(S)
       2: STEP WIDTH (S)
       3: FLUX THROUGH FRONT SURFACE
       4: INTEGRAL OF BULK CONCENTRATION
       5: FLUX THROUGH REAR SURFACE
```

Note again that all quantities are calculated in atomic units; fluxes, fluences and areal densities must be multiplied by the host atomic density in order to obtain the common dimensions.

An evaluation program which performs plots of the results is available on the PWW PDP 11/60 computer.

Appendix C: Batch Input Example

The first line of the batch stream contains the maximum run time and the output switches PR, PU, and PU1, which are normally either 10 (PDP 11/6Ø PWW) or 13 (AMOSPRNT or AMOSPNCH files). PR refers to the control output, PU to the main output and PU1 to the optional DUMP output.

In this example, the input data consist of the parameter set (example in App. B), a dump file from a previous calculation for the initial concentrations, and an x-y data set for the source distribution.

```
/JOB R=1ØØ T=ØØØ:2Ø PR=13 PU=1Ø PU1=13
ASSIGN(DN=$PUNCH,A=FTØ7)
ASSIGN(DN=$PUNCH1,A=FT17)
CFT,L=Ø,OFF=P,ON=Z.
LDR,MAP=Ø,SET=INDEF.
EXIT.
DUMPJOB.
DEBUG,TRACE.
/EOF
$$ WDM:F.PIDVC
$$ WDM:F.GERB4C
$$ WDM:D.ERF
/EOF
$$ PRB:F.DATIC
$$ PRB:AMOSPNCH.PRB381
$$ PRB:B.TRI133
/EOF
```